Intratracheal transplantation of mesenchymal stem cells simultaneously attenuates both lung and brain injuries in hyperoxic newborn rats

Young Eun Kim[1], Won Soon Park[1,2,3], Dong Kyung Sung[2,3], So Yoon Ahn[2,3], Se In Sung[2], Hye Soo Yoo[2] and Yun Sil Chang[1,2,3]

BACKGROUND: Bronchopulmonary dysplasia is an independent risk factor for adverse neurodevelopmental outcomes in premature infants. We investigated whether attenuation of hyperoxic lung injury with intratracheal transplantation of human umbilical cord blood-derived mesenchymal stem cells (MSCs) could simultaneously mitigate brain damage in neonatal rats.

METHODS: Newborn Sprague-Dawley rats were exposed to hyperoxia or normoxia conditions for 14 d. MSCs (5×10^5 cells) were transplanted intratracheally at postnatal day (P) 5. At P14, lungs and brains were harvested for histological and biochemical analyses.

RESULTS: Hyperoxic lung injuries, such as impaired alveolarization evident from increased mean linear intercept (MLI) and elevated inflammatory cytokine levels were significantly alleviated with MSC transplantation. Hyperoxia decreased brain weight, increased brain cell death, and induced hypomyelination. MSC transplantation significantly ameliorated hyperoxia-induced increased terminal deoxynucleotidyl transferase dUTP nick end labeling (TUNEL)-positive cells in the dentate gyrus and reduced myelin basic protein. In correlation analyses, brain weight and myelin basic protein (MBP) were significantly inversely correlated with lung MLI and inflammatory cytokines, while TUNEL-positive brain cell number showed a significant positive correlation with lung MLI.

CONCLUSION: Despite no significant improvement in short-term neurofunctional outcome, intratracheal transplantation of MSCs simultaneously attenuated hyperoxic lung and brain injuries in neonatal rats, with the extent of such attenuation being closely linked in the two tissues.

Bronchopulmonary dysplasia (BPD), a chronic lung disease that occurs in premature infants receiving prolonged ventilator support and oxygen supplementation, is associated with an increased risk of long-term neurodevelopmental impairments (1). Despite its limited predictive value, some clinical studies have also identified BPD as an independent risk factor for the development of neurofunctional deficits in premature infants, including cerebral palsy and developmental retardation, even in the absence of catastrophic brain injuries such as intraventricular hemorrhage and hypoxic-ischemic encephalopathy (1–3). No specific or effective treatment is currently available for the preterm infant brain. However, as indicated by evidence from Pham *et al.* (4), the close association between BPD and brain injury suggests that pulmo-protective therapies might also be neuroprotective in premature infants.

Recently, we reported that intratracheal xenotransplantation of human umbilical cord blood (UCB)-derived mesenchymal stem cells (MSCs) significantly attenuated hyperoxia-induced lung injuries in immune-competent newborn rats (5–7). Furthermore, in a phase I clinical trial, we showed that intratracheal transplantation of allogenic human UCB-derived MSCs in very preterm infants is safe and feasible (8). However, beyond its pulmo-protective properties, the potential neuroprotective effects of intratracheal MSCs transplantation have not yet been evaluated. In the present study, we used a newborn rat model of prolonged postnatal exposure to hyperoxia to develop neonatal hyperoxic lung and brain injuries, simulating clinical BPD and associated brain injury in very preterm infants. We tried to determine whether intratracheal MSC transplantation could simultaneously attenuate both lung and brain injuries, and whether the extent of such attenuation was correlated in these two tissues in hyperoxic newborn rats.

RESULTS

Survival Rate, and Body and Brain Weight

Exposure to hyperoxia significantly reduced survival rate at postnatal day (P) 14 from 100% in the normoxia control (NC) group to 76% in the hyperoxia control (HC) group. The 87% survival rate observed in the hyperoxia with MSC transplantation (HM) group was not significantly different from the NC group.

Although birth weights did not differ significantly between the three study groups, body (24.69 ± 1.06 g) and brain weights (1.07 ± 0.02 g) of HC rats at P14 were significantly lower than those of NC rats (28.01 ± 0.42 and 1.16 ± 0.02 g, respectively). Body and brain weights at P14 (26.05 ± 0.78 and 1.10 ± 0.01 g, respectively) in the HM group were not significantly different from the NC group. However, the apparent increase in body and brain weight

The first two authors are the co-first authors of this work.

[1]Department of Health Sciences and Technology, Samsung Advanced Institute for Health Sciences and Technology (SAIHST), Sungkyunkwan University, Seoul, Korea; [2]Department of Pediatrics, Samsung Medical Center, Sungkyunkwan University School of Medicine, Seoul, Korea; [3]Stem Cell and Regenerative Medicine Center, Research Institute for Future Medicine, Samsung Medical Center, Seoul, Republic of Korea. Correspondence: Yun Sil Chang (cys.chang@samsung.com)

Received 30 June 2015; accepted 20 February 2016; advance online publication 11 May 2016. doi:10.1038/pr.2016.88

in the HM group compared to the HC group did not reach statistical significance (Figure 1a,b). The brain/body weight ratio (%) was not significantly different between NC, HC, and HM (NC: 4.12 ± 0.07, HC: 4.37 ± 0.20, HM: 4.34 ± 0.13) (Figure 1c).

Histological and Morphometric Analysis of P14 Rat Lungs

Representative light microscopy photomicrographs showing histopathological differences between the study groups are shown in Figure 2a. While small and uniform alveoli were observed in NC rat lungs, the HC group displayed fewer, larger, heterogeneously sized, and corrugated alveoli, indicative of impaired alveolarization. These hyperoxia-induced morphological changes and impairments in alveolar development were attenuated in the HM group. Morphometric analysis revealed that the mean linear intercept (MLI), an indication of alveolar size, was significantly higher in HC rats (72.5 ± 2.3 μm) compared to NC rats (52.7 ± 1.3 μm). This increased MLI was significantly attenuated in the HM group (63.5 ± 1.6 μm) (Figure 2b).

Inflammatory Cytokines, VEGF, and Superoxide Dismutase

Lung cytokines such as tumor necrosis factor (TNF)-α, interleukin (IL)-1α, IL-1β, and IL-6 were significantly increased and vascular endothelial growth factor (VEGF) was significantly decreased in the HC group compared to the NC group. These hyperoxia-induced effects were significantly diminished by MSC transplantation in HM rats (Figure 3a,b).

In contrast, no significant differences in brain cytokine levels measured at P2, P6, and P14 (**Supplementary Figure S1** online) and brain superoxide dismutase activity, measured at P14 (**Supplementary Figure S2** online), were observed between the study groups.

TUNEL- and Ectodermal Dysplasia 1-Positive Brain Cells

Representative photomicrographs of terminal deoxynucleotidyl transferase dUTP nick end labeling (TUNEL), ectodermal dysplasia (ED) 1 and ionized calcium binding adaptor molecule (Iba)-1-positive cells in the periventricular zone (PVZ), hippocampal dentate gyrus (DG), and cortex, are shown in Figure 4a–c and **Supplementary Figure S3a–c** online, respectively. The number of TUNEL-positive cells in the brains of HC rats was significantly increased compared to the NC group. This hyperoxia-induced increase in TUNEL-positive cells in the DG was significantly mitigated by MSC transplantation, as seen in the HM group. In addition, the number of TUNEL-positive cells in the cortex did not significantly differ between the HM and NC groups (Figure 4d–f). On the other hand, MSC transplantation did not cause any changes in the number of TUNEL-positive brain cells in the normoxic animals (**Supplementary Figure S4a–c,e–g** online).

There were no significant differences in the number of ED1-positive cells (Figure 4g–i), and Iba-1-positive cells (**Supplementary Figure S3d–f** online), indicating active and total microglial cells, respectively, between the study groups.

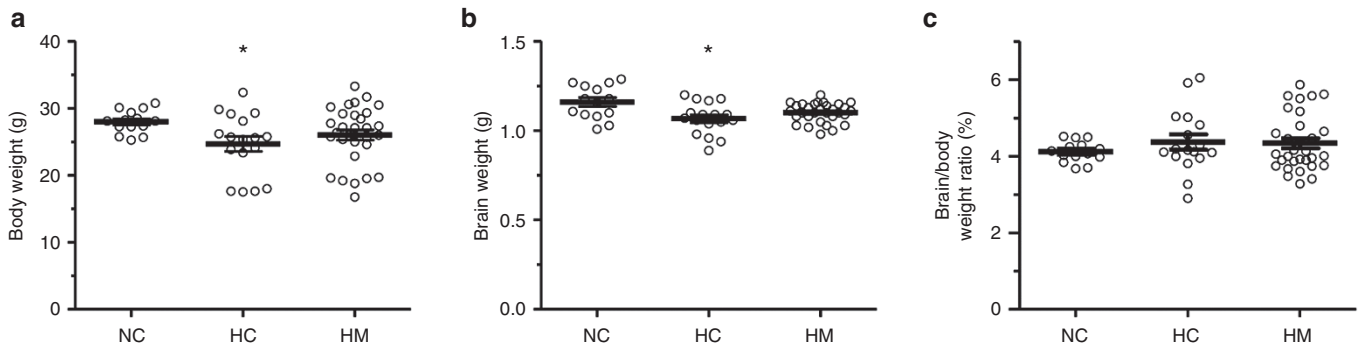

Figure 1. Body and brain weights. (**a**) Body weight, (**b**) brain weight, and (**c**) brain/ body weight ratio (%) at postnatal day (P) 14 of NC, HC, and HM rats exposed to 21% (normoxia) or 90% (hyperoxia) oxygen for 14 d. Data are given as mean ± SEM. *$P < 0.05$ vs. NC. HC, hyperoxia control; HM, hyperoxia with intratracheal transplantation of umbilical cord blood-derived mesenchymal stem cells; NC, normoxia control.

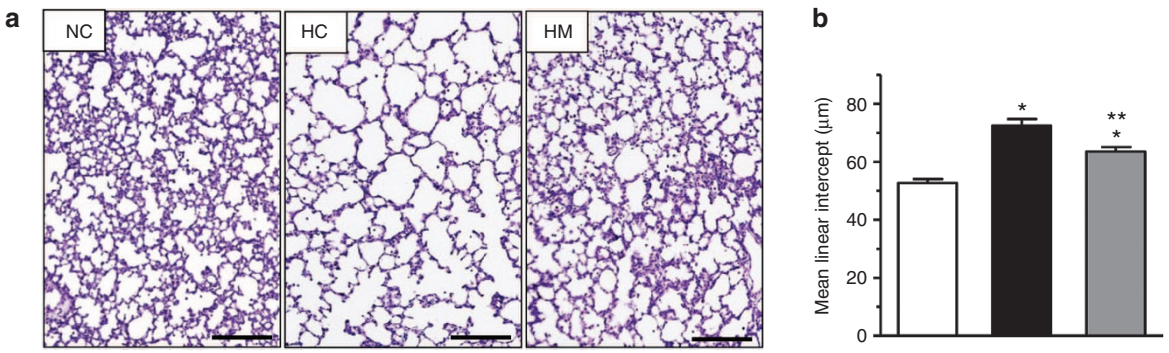

Figure 2. Morphometric assessment of alveolarization. (**a**) Representative photomicrographs of lungs stained with hematoxylin and eosin (scale bar, 100 μm) at a magnification of 200 ×. (**b**) Morphometric measurements of mean linear intercepts (μm). White bar: normoxia control (NC); black bar: hyperoxia control (HC); gray bar: HM. Data are given as mean ± SEM. *$P < 0.01$ vs. NC. **$P < 0.01$ vs. HC.

Brain Caspase-3 Levels and Oxidative Stress

Representative western blots for caspase-3 and carbonylated protein in brain homogenates at P2, P4, P6, P8, and P14, respectively are shown in **Figure 5a**. Caspase-3 levels (**Figure 5a,b**) in the brain were significantly increased in the HC group compared to the NC group at all time points, and these increases were significantly attenuated after MSC transplantation, as seen in the HM group (**Figure 5b**). Brain oxidative stress, assessed by

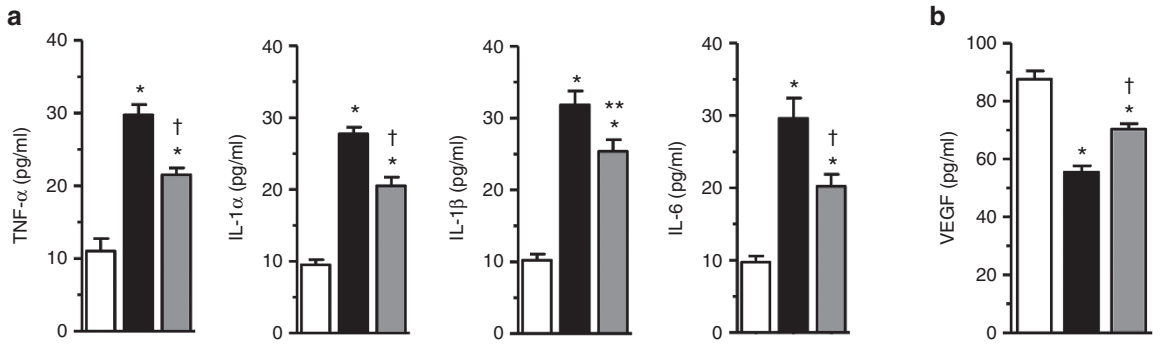

Figure 3. Inflammatory cytokines in the lungs. Levels of (**a**) TNF-α, IL-1α, IL-1β, IL-6, and (**b**) vascular endothelial growth factor measured in lung tissue. White bars: normoxia control (NC); black bars: hyperoxia control (HC); gray bars: HM. Data are represented as mean ± SEM. *$P < 0.01$ vs. NC. **$P < 0.05$ vs. HC. †$P < 0.01$ vs. HC.

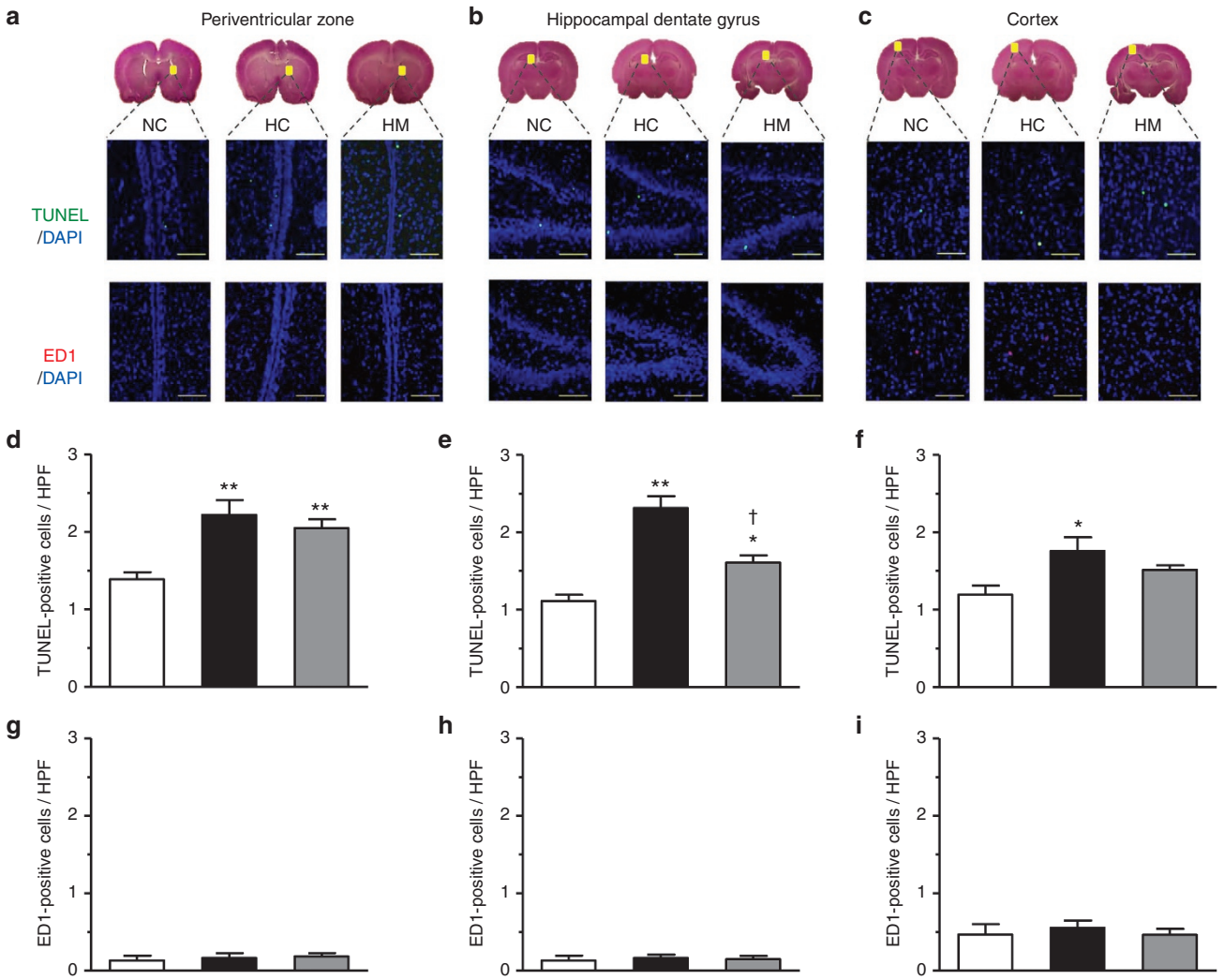

Figure 4. Dead cells and activated microglia in brain tissue. (**a–c**) Representative fluorescence micrographs of brain tissue stained with TUNEL (green), ED1 (red), and 4′,6-diamidino-2-phenylindole (DAPI; blue) in the periventricular zone, hippocampal dentate gyrus, and cortex at P14. Images were taken at a magnification of 200× (scale bar, 100 μm). The number of (**d–f**) TUNEL-positive cells and (**g–i**) ED1-positive microglia per high-power field is shown in each brain region. White bars: normoxia control (NC); black bars: HC; gray bars: HM. Data are given as mean ± SEM. *$P < 0.05$ vs. NC. **$P < 0.01$ vs. NC. †$P < 0.01$ vs. HC.

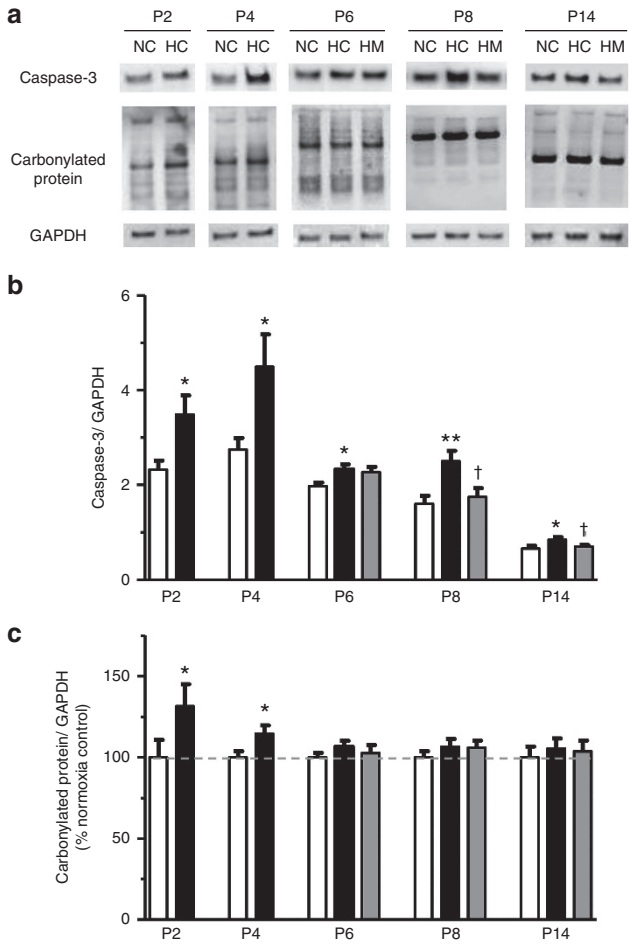

Figure 5. Western blots for Caspase-3 and carbonylated protein in brain homogenates at P2, P4, P6, P8, and 14. (**a**) Representative western blots of Caspase-3 (top), carbonylated protein (mid) and glyceraldehyde-3-phosphate dehydrogenase (GAPDH) (bottom; loading control). (**b**) Densitometric analysis of caspase-3 levels normalized to GAPDH. (**c**) Densitometric analysis of carbonylated protein levels normalized to GAPDH, given as percentage of normoxia control (NC) group at each corresponding time points. White bars: NC; black bars: HC; gray bars: HM. Data are mean ± SEM. *$P < 0.05$ vs. NC. **$P < 0.01$ vs. NC. †$P < 0.05$ vs. HC. ($n = 6$ per group).

carbonylated protein contents, was significantly increased at the early time points of P2 and P4, but not thereafter, at P6, P8, and P14 in the HC group compared to the NC group (**Figure 5c**).

Brain Myelination

Brain myelination was assessed via immunofluorescent staining for myelin basic protein (MBP) at P14 (**Figure 6**). MBP fluorescence intensity, indicative of the extent of brain myelination, was significantly reduced in the HC group compared to the NC group, but no difference was detected between the HM and NC groups. In addition, there was no difference in MBP fluorescence intensity between normoxic groups without MSC transplantation (NC) or with MSC transplantation (NM) (**Supplementary Figure S4d,h** online).

In western blot analysis, level of proteoglycan nerve-glia antigen 2 (NG2), a marker for immature oligodendrocyte progenitor cells, and levels of MBP, a marker for mature oligodendrocyte were evaluated at P8 and P14, because brain myelination typically begins to develop at around P7 in neonatal rats (9). Levels of NG2 and MBP were significantly reduced at P8 and P14 in the HC group compared to the NC group. However, in the HM group, these reduced NG2 levels were restored at P8 and P14, and MBP levels were restored at P14 compared to the HC group (**Figure 6d–f**).

Short-Term Neurofunctional Outcome

Developmental reflexes such as the righting reflex at P11–13 and negative geotaxis at P14 were done to assess short-term neurofunctional outcome (10,11). A significant delay in the maturation of righting reflex, as well as retardation of negative geotaxis, was observed in the HC group compared with the NC group. Although the HM group appeared to show some improvement on these measures, the effects did not reach statistical significance (**Supplementary Figure S5** online).

Presence of Donor Cells

At P6 and P8, after intratracheal transplantation of MSCs, expression of human glyceraldehyde-3-phosphate dehydrogenase, indicative of the presence of human RNA derived from donor human MSCs, was detected only in the lung tissue, whereas not detected in the brain tissue of the HM group (**Supplementary Figure S6** online).

Correlation Analysis of Lung and Brain Injuries

Lung MLI showed a significant inverse correlation with brain weight ($R^2 = 0.072$, $P = 0.036$; **Figure 7a**) and brain MBP fluorescence ($R^2 = 0.146$, $P = 0.034$; **Figure 7b**), a significant positive correlation with TUNEL-positive cell number in the PVZ ($R^2 = 0.397$, $P < 0.001$; **Figure 7c**) and DG ($R^2 = 0.362$, $P < 0.001$; **Figure 7d**), but not in the cortex ($R^2 = 0.095$, $P = 0.092$; **Figure 7e**), and no significant correlation with body weight ($R^2 = 0.041$, $P = 0.113$; **Figure 7f**). The inflammatory cytokines TNF-α, IL-1α, IL-1β, and IL-6 showed significant inverse correlations with brain weight ($R^2 = 0.197$, $P = 0.012$; $R^2 = 0.359$, $P < 0.001$; $R^2 = 0.281$, $P = 0.002$; $R^2 = 0.165$, $P = 0.02$, respectively; **Figure 8a–d**), and VEGF showed significant positive correlation with brain weight ($R^2 = 0.319$, $P = 0.001$; **Figure 8e**).

DISCUSSION

We previously observed that intratracheal transplantation of human UCB-derived MSCs improved hyperoxic lung injuries in newborn rats (5–7), and the clinical application of MSCs transplantation to the very premature infants is safe and feasible (8). In the present study, we asked whether intratracheal transplantation of MSCs could attenuate not only hyperoxic lung injury but also hyperoxic brain damage in newborn rats. In accordance with our previous studies (5–7), we observed that intratracheal transplantation of human UCB-derived MSCs significantly attenuated hyperoxia-induced lung injuries, including increased MLI, indicating impaired alveolarization, elevated levels of lung inflammatory cytokines, and

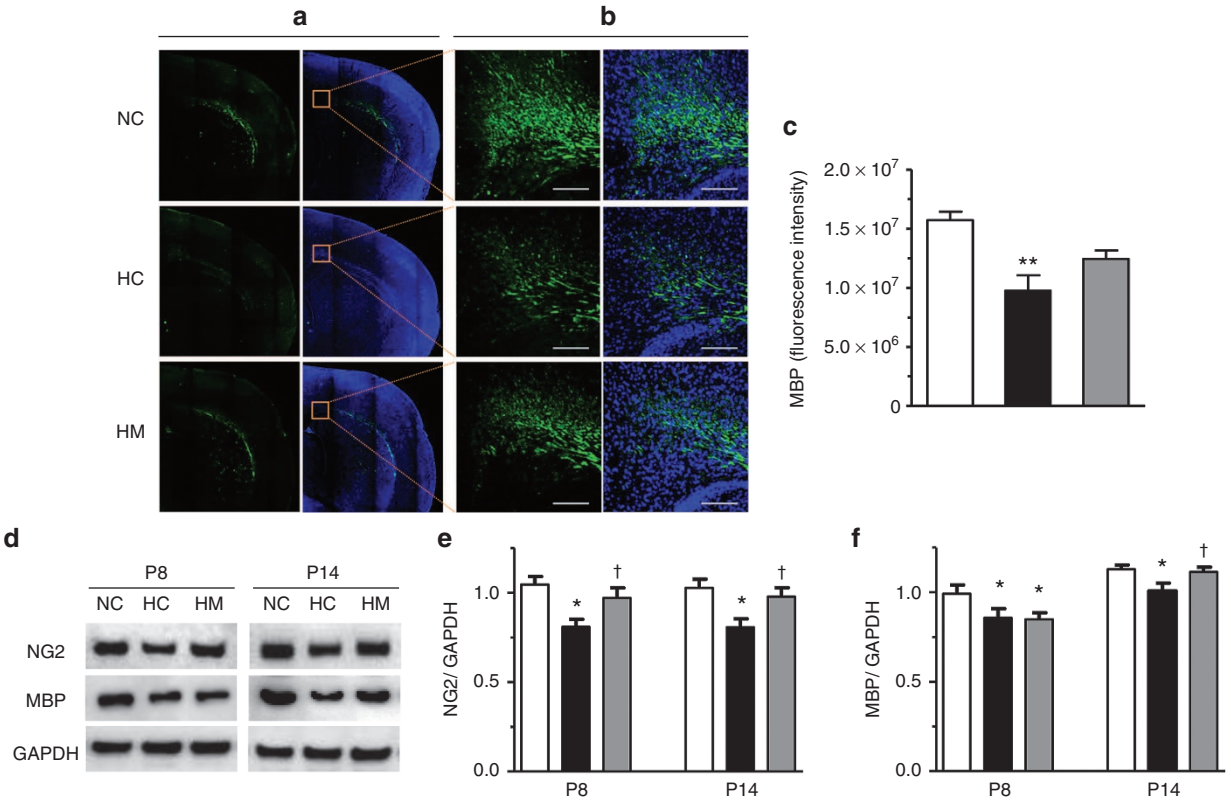

Figure 6. Myelin basic protein (MBP)-positive nerve fibers and neural/glial antigen 2 (NG2)-positive cells in brain tissue. (**a**) Representative tile-scan confocal images of brain tissue stained for MBP (green) and with 4′,6-diamidino-2-phenylindole (DAPI; blue) in white matter areas, including the lateral corpus callosum, cingulum, and external capsule, for each group at P14. (**b**) Magnified images of the rectangular boundary of the cingulate white matter area taken at a magnification of 100 × (scale bar, 200 μm). (**c**) Average myelin basic protein (MBP) fluorescence intensity in cingulate white matter. (**d**) Representative western blots of NG2 and MBP. (**e**) Densitometric analysis of NG2 levels normalized to glyceraldehyde-3-phosphate dehydrogenase (GAPDH). (**f**) Densitometric analysis of MBP levels normalized to GAPDH. White bars: normoxia control (NC); black bars: HC; gray bars: HM. Data are given as mean ± SEM. *$P < 0.05$ vs. NC. **$P < 0.01$ vs. NC. †$P < 0.05$ vs. HC.

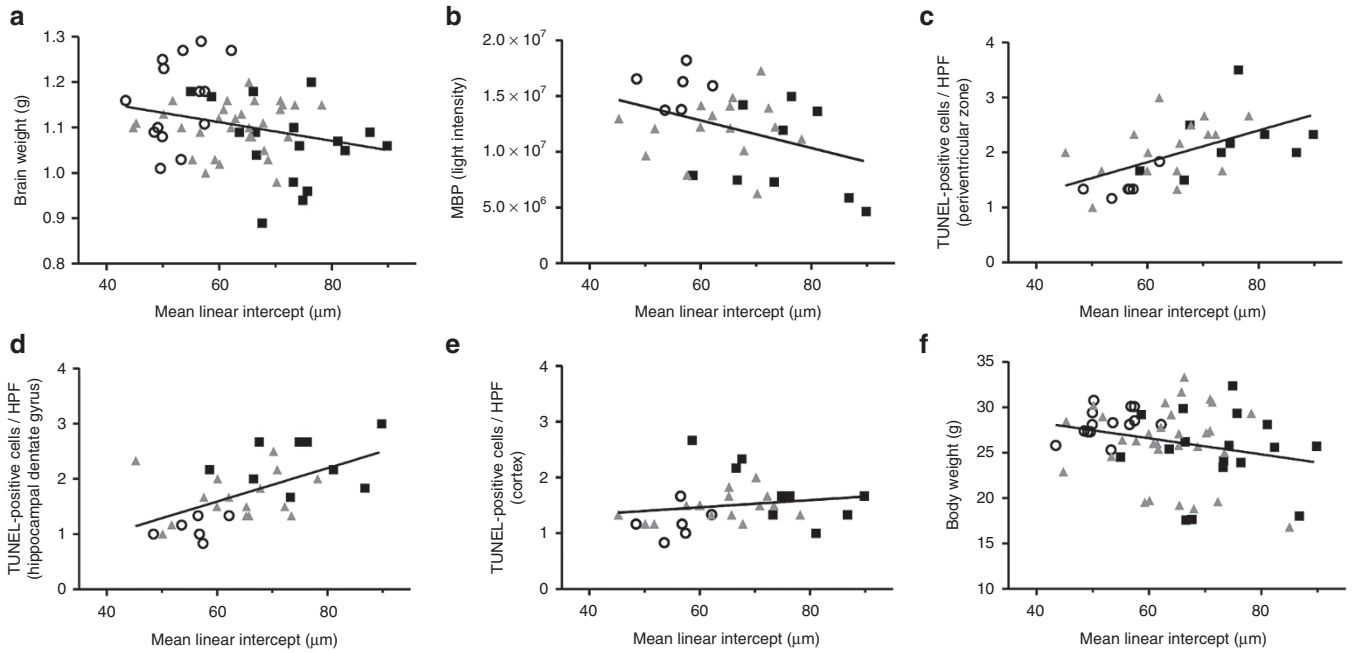

Figure 7. Correlation analyses of lung alveolarization and brain characteristics. X-axes: (**a–f**) Mean linear intercept (μm). Y-axes: (**a**) brain weight (in grams) ($R^2 = 0.072$, $P = 0.036$), (**b**) fluorescence intensity of myelin basic protein in cingulate white matter ($R^2 = 0.146$, $P = 0.034$), (**c–e**) number of TUNEL-positive cells per high-power field in the periventricular zone, hippocampal dentate gyrus, and cortex, respectively ($R^2 = 0.397$, $P < 0.001$; $R^2 = 0.362$, $P < 0.001$; $R^2 = 0.095$, $P = 0.092$, respectively), and (**f**) body weight (in grams) ($R^2 = 0.041$, $P < 0.113$). White circles: normoxia control, black squares: HC, and gray triangles: HM.

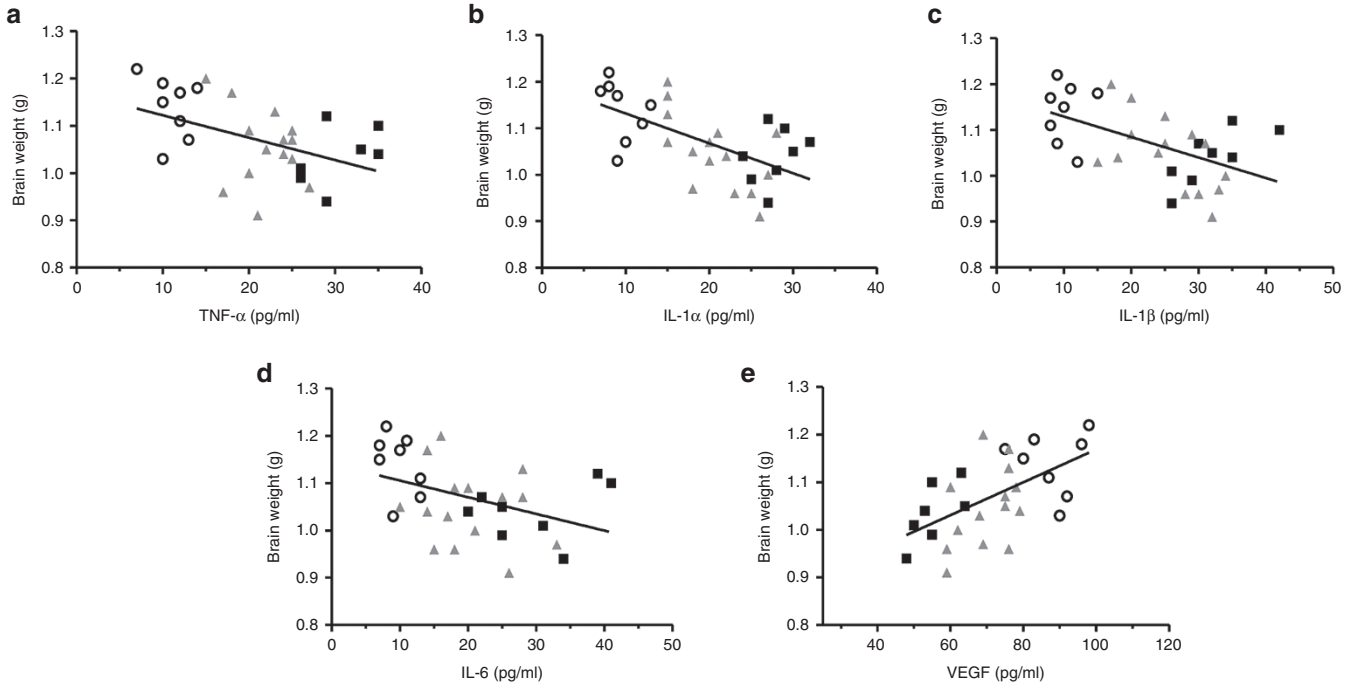

Figure 8. Correlation analyses of lung characteristics and brain weight. Y-axes: (**a–e**) brain weight (in grams). X-axes: (**a–d**) lung inflammatory cytokine concentrations (pg/ml), including TNF-α, IL-1α, IL-1β, and IL-6, respectively ($R^2 = 0.183$, $P = 0.017$; $R^2 = 0.289$, $P < 0.002$; $R^2 = 0.241$, $P = 0.005$; $R^2 = 0.179$, $P = 0.018$, respectively), and (**e**) vascular endothelial growth factor concentration (pg/ml) ($R^2 = 0.319$, $P < 0.001$). White circles: normoxia control, black squares: HC, and gray triangles: HM.

reduced presence of VEGF. Simultaneously, MSC transplantation mitigated hyperoxic brain injuries, such as increased TUNEL positive cells in dentate gyrus as well as increased caspase-3 expression in whole brain and white matter injury evidenced by reduced MBP. To our knowledge, this is the first report of simultaneous neuroprotective effects of local intratracheal transplantation of MSCs for BPD in hyperoxic newborn rats. Taken together, these findings suggest that hyperoxic brain injury is closely connected to BPD, and that intratracheal transplantation of MSCs could go beyond mere attenuation of this condition to simultaneously improve associated brain injury and poor neurodevelopmental outcomes in very preterm infants.

The use of oxygen is critical for neonatal intensive care, and premature infants are especially vulnerable to oxygen toxicity due to the high possibility of exposure to supra-physiological oxygen concentrations during resuscitation and respiratory management, and a highly immature antioxidant defense mechanism. Besides the well-known toxic effects of hyperoxia on the developing lung, hyperoxia also leads to cell death in the developing white and grey matter of the brain, resulting in motor and cognitive deficits in premature infants (12–15). In addition to the lung injury known to occur after prolonged exposure to hyperoxia (90% oxygen for 14 d), our data revealed simultaneous hyperoxic brain injury, shown by a retardation in brain weight gain, transiently increased carbonylated protein, reduced MBP, and an increased TUNEL-positive cells and caspase-3 expression, without changes in inflammatory cytokine levels, the number of activated microglia, and superoxide dismutase activity. These observations indicate that the newborn rat model used in this study appropriately simulates the clinical conditions of BPD with associated brain injury in premature infants (4,16).

The mechanism by which local intratracheal transplantation of MSCs confers a neuroprotective effect, despite the absence of MSCs in the brain, remains unclear. In a multicenter clinical study (1,12), only very-low-birth-weight infants with BPD requiring prolonged oxygen supplementation were at higher risk of poor long-term neurocognitive and academic performance, compared to premature infants exhibiting less severe BPD. These findings suggest that only severe BPD constitutes an independent risk factor for associated brain injury and poor long-term neurodevelopmental outcome in very-low-birth-weight infants (1,17). Besides hyperoxia, infection and inflammation have also been implicated in preterm infant brain injury (18,19). In the present study, lung MLI, an indicator of alveolarization, showed a significant negative correlation with brain weight and MBP, and a significant positive correlation with the number of TUNEL-positive cells in the brain, measured at P14. Lung inflammatory cytokines and VEGF levels showed significant positive and negative correlations with brain weight, respectively, at P14. We have shown that the protective effects of MSC transplantation may primarily be mediated by a paracrine rather than a regenerative mechanism, and have highlighted the critical role of growth factors, including VEGF, in mediating the antioxidative, anti-inflammatory, and antiapoptotic paracrine effects of MSC transplantation (20). Taken together, these findings suggest that the neuroprotective

effects of intratracheal MSC transplantation might be mediated by a multitude of factors, including the attenuation of hyperoxic lung injury itself, anti-inflammatory, antioxidative, and antiapoptotic paracrine effects, and growth factors, such as VEGF.

Hyperoxic injury in the developing brain is maturation-dependent, causing caspase-dependent apoptosis in immature and preoligodendrocytes, but not in mature oligodendrocytes (21). Furthermore, rats at P3 and P6, but not at P10, showed hypomyelination upon exposure to 80% oxygen (15). In the study by Vottier *et al.* (22), white matter myelin content and mature oligodendrocyte density at P10 were significantly reduced by postnatal hyperoxia for 7 d, but >2-fold increase in ED1- and TUNEL-positive cells at P3 tended to subside at P10, and significantly increased GFAP positive cells at P3 became normalized at P10. There were no significant differences in several neurotrophic factors, such as BDNF and VEGF, between the study groups. Overall, these findings suggest that hyperoxia induced brain injury occurs primarily during the most vulnerable developmental period, i.e., first postnatal week of life (14,15), comparable to human gestational age of 23–32 wk (23). In addition, the maturation of the antioxidant enzymes by P14 in rats could protect the newborn brain from oxidative stress and ensuing inflammation (24). In the present study, increased caspase-3 levels, which was persistently elevated between P2 and P14 in hyperoxic brains, was significantly attenuated at P8 and 14 by intratracheal MSC transplantation at P5. Caspase-3 is a key marker for apoptosis (25), but not specific because it is also involved in other metabolic processes (26). Therefore, performing simultaneous and serial evaluation of not only caspase-3 but also other apoptotic marker such as TUNEL would be more appropriate for the exact assessment of brain cell death. The lack of of additional serial assessment of other apoptotic cell markers is one of the limitations of the present study. Intratracheal MSC transplantation also ameliorated white matter injury in hyperoxic animals, preserving immature oligodendrocyte progenitor cells evident from increased NG2 level at P8 and 14, and, subsequently, preserving mature oligodendrocytes evident from increased MBP at P14.

Oxidative stress in the hyperoxic brain, marked by increased carbonylated protein, was only transiently increased at P2 and P4, before MSC transplantation, and returned to baseline levels thereafter, thus precluding demonstration of a direct antioxidative mechanism. Superoxide dismutase activity also did not differ between normoxic and hyperoxic brains. Given that there were no increases of inflammatory cytokines in hyperoxic brains, direct anti-inflammatory protection mechanisms could not be considered or evaluated. Moreover, MSCs transplanted were not detected in the brain. Therefore, we speculate that the neuroprotective mechanisms of intratracheally transplanted MSCs may be indirect as follows. First, intratracheally transplanted MSCs may indirectly affect the developing hyperoxic brain, via an improved systemic milieu associated with decreasing oxidative stress and inflammation in hyperoxic lungs. This is supported by evidence of a significant correlation of lung cytokine levels with brain weight as well as the number of brain TUNEL-positive cells, which may reflect that significant amelioration of hyperoxic brain injuries might associate with significant attenuation of systemic, and lung oxidative stress and ensuing inflammation by MSC transplantation. Second, paracrine factors, which are secreted from intratracheally transplanted MSCs, then entering systemic circulation, might play a direct protective role against increased cell death in the developing hyperoxic brain. The maturation of blood–brain barrier (BBB) is developmental and time dependent in neonatal rat (27). Furthermore, oxidative stress (28) and inflammation (29) have been shown to compromise the BBB function especially during the early developmental period. Wei *et al.* (30) have reported that the conditioned media of adipose stromal cells protect against hypoxia–ischemia-induced brain damage in P7 neonatal rats. They have showed that the factors within the conditioned media penetrated the BBB, which was disrupted by the inflammatory response after hypoxic–ischemic injury. Therefore, possible neuroprotective mechanism in our experiment could be through paracrine factors from intratracheally transplanted MSCs that enter into the systemic circulation and cross the BBB, which is relatively immature and probably disrupted by prolonged hyperoxia, in neonatal rat. However, to verify this, further studies are needed as the next step. Taken together, to clarify these neuroprotective mechanisms is necessary and future studies are needed. As some regions of the brain might be more vulnerable to hyperoxia than others, we measured TUNEL- and ED1-positive cells in brain through specific three regions, PVZ, DG, and parietal cortex. First, PVZ is known to be one of the most vulnerable regions to hyperoxic stress (31). Second, DG plays a critical role in learning and memory and neuroblasts reside, proliferate, and migrate (31) in its subgranular layer, and the cortex is neuron-rich gray matter, in which neurons process sensory information and generate fine motor skills (32). According to the previous reports (33), parietal cortex is also a region vulnerable to hyperoxia-induced cell death.

Besides attenuating abnormal histopathology, improving functional outcomes is crucial for the clinical application of MSCs in the premature infants. However, there is no consensus regarding the reliability of short-term neurodevelopmental effects of hyperoxic brain injury in the newborn rats up to P14. In the present study, hyperoxia (HC) retarded the maturation of righting reflex tested at P11-13 and slowed negative geotaxis tested at P14. Ostensible improvements in the HM group did not reach statistical significance. These findings suggest that short-term neurodevelopmental assessment is nonspecific, and may not be sensitive enough to detect the histopathologic improvements. Long-term neurodevelopmental studies, including the rotarod and water maze tests, will be necessary to assess the relevance of histopathology to behavior (34–36).

Optimizing MSC transplantation timing for hyperoxic lung and brain injuries is an important issue in clinical translation. Hyperoxic brain damage in rodents is age-dependent, with maximum vulnerability occurring during the first week of life (14,15). In our previous work (5), we showed that intratracheal transplantation of MSCs attenuated hyperoxic lung injury in newborn rats in a time-dependent manner, conferring significant protection in the early (P3), but not late (P10), phase of inflammation. These

findings suggest that the therapeutic time window available for MSC transplantation may be narrow for BPD and hyperoxia-associated brain injury in preterm infants; further work will be necessary to define this critical window.

Successful clinical translation also requires understating of the optimal route of MSC transplantation. In the present study, MSCs were delivered intratracheally based on our previous preclinical studies showing >4-fold more potent therapeutic efficacy compared with systemic intraperitoneal (7) or intravenous transplantation (37). Intravenously transplanted MSCs do not cross the blood brain barrier, and are trafficked not only in the pulmonary capillaries but also in other organs, such as the liver, spleen, and kidney (38). Moreover, human umbilical mononuclear cells given intravenously did not attenuate excitotoxic white matter injury, and even aggravated white matter lesion following intraperitoneal administration (39). Overall, these findings indicate that local intratracheal route might be more efficient than the systemic intravenous route for MSC transplantation in an animal model of combining developing lung and brain injuries, simulating BPD and white matter damage in preterm infants.

In summary, by using a newborn rat model of prolonged exposure to hyperoxia in this study, we were able to induce both lung and brain injuries, simulating clinical BPD and associated brain injury in very premature infants. We also demonstrated that intratracheal transplantation of MSCs in hyperoxic infant rats significantly reduced not only lung injuries, but also associated brain damage and this attenuation was closely linked in the two tissues.

METHODS

Cell Preparation

This study was approved by the Institutional Review Board of Samsung Medical Center and Medipost, Seoul, Korea. As described previously (5–7), MSCs were isolated from human UCB after neonatal delivery and informed consent was received from donors. UCB-derived MSCs were cultivated and confirmed for their characteristics using previously established protocols (5–7).

Animal Model

The Animal Care and Use Committee of the Samsung Biomedical Research Institute (Seoul, Korea) reviewed and approved the experimental protocol described herein. This study also followed the Institutional and National Institutes of Health guidelines for laboratory animal care. As described previously (5–7), timed pregnant Sprague-Dawley rats (Orient, Seoul, Korea) were housed in individual cages with free access to water and laboratory chow. Within 10 h after birth, the newborn rat pups were divided into three groups: normoxia control (NC; $n = 14$); hyperoxia control (HC; $n = 17$); and hyperoxia with intratracheal MSC transplantation (HM; $n = 31$). Normoxic rat pups were kept in room air, while hyperoxic rats were raised in hyperoxic chambers (90% oxygen) from birth until P14. To investigate the effect of MSC transplantation on normoxic control animals, a group of normoxic rats with intratracheal MSC transplantation (NM; $n = 6$) was added. In order to evaluate serial hyperoxic brain injury, time course experiments were done separately and animals were sacrificed as follows: the NC and HC groups at P2, P4, P6, P8, and P14, and HM group at P6, P8, and 14 respectively ($n = 6$ in each group). The details of hyperoxic exposure have been described previously (6,7).

Transplantation of Human UCB-Derived MSCs

For transplantation, fifth-passage human UCB-derived MSCs from a single donor were used. At P5, 5×10^5 MSCs in 0.05 ml normal saline (NS) were intratracheally transplanted into HM rats, while an equal volume of NS was intratracheally administered to NC and HC animals. No mortality occurred during the transplantation procedure. Details of this procedure, as well as transplantation of MSCs have been described previously (5–7).

Tissue Preparation

At P14, under deep pentobarbital anesthesia (60 mg/kg, i.p.), the lung and brain were harvested immediately following transcardiac perfusion with ice-cold NS. Rat brains were extracted wholly from olfactory bulbs to cerebellum, and the whole brain was weighed to an accuracy of two decimal places with an electronic scale guaranteed weight ranging from 0.20 to 400 g with 0.01 g readability (Scout Pro; OHAUS, Parsippany, NJ). Extracted lung tissue for morphometric analyses was inflated with NS and then immersion-fixed as previously (6,7). For histological analysis of both lung and brain in each rat ($n = 6$–16 per group), harvested tissues were fixed in 10% buffered formalin (40) before being embedded in paraffin wax the following day. Paraffin blocks of lung and brain tissues were then sliced into 4 μm sections. For biochemical observations ($n = 8$–15 per group), the lung and brain were snap frozen in liquid nitrogen and stored at −80 °C until use.

Lung Morphometry

The level of lung alveolarization was evaluated by MLI, representing mean interalveolar distance, using hematoxylin and eosin-stained lung sections, as described previously (5–7). MLI was measured as described by Cooney and Thurlbeck (41). A minimum of two sections per rat and six fields per section were examined randomly for each analysis.

Enzyme-linked immunosorbent assay

Following homogenization and centrifugation of frozen lung and brain tissues, the protein concentration in each supernatant was standardized across all samples. The levels of TNF-α, IL-1α, IL-1β, IL-6, and VEGF were measured using a MILLIPLEX MAP ELISA Kit according to the manufacturer's protocol (EMD Millipore, Billerica, MA).

TUNEL Assay

Apoptosis was assayed via fluorescent TUNEL staining of brain sections (n= 6, 9, and 16 in NC, HC, and HM, respectively, and $n = 6$ in NM). Detailed materials and methods for counting TUNEL-positive cells are provided in the **Supplementary Methods** online.

Immunohistochemistry

To detect myelination, coronal brain sections were immunostained for MBP by incubation with an anti-MBP primary antibody (1:500; Abcam, Cambridge, UK) and an anti-mouse IgG secondary antibody (1:500; Invitrogen, Eugene, OR). To detect activated microglia, sections were immunostained for ED1 by incubation with an anti-monocyte/macrophage primary antibody (1:250; Millipore, Bedford, MA) and an anti-mouse IgG secondary antibody (1:500; Invitrogen). Total microglia, including activated and resting forms, were stained with Iba-1 antibodies. Brain sections were incubated with anti Iba-1 primary antibody (1:200; Abcam, Cambridge, UK) and anti-goat IgG secondary antibody (1:200; Invitrogen). Detailed materials and methods for observing MBP-positive nerve fibers, ED1-positive cells, and Iba-1-positive cells are provided in the **Supplementary Methods** online.

Western Blot

Carbonylated protein, caspase-3, Neural/glial antigen 2 (NG2), and MBP in whole brains were detected by western blot. Protein Carbonyl Western Blot kit (Cosmo Bio, Tokyo, Japan) was used according to the manufacturer protocol to detect carbonylated protein content, a biomarker of oxidative stress. To detect caspase-3, NG2 and MBP levels, the membranes were blocked and incubated with caspase-3 primary antibody (1:1,000; Cell Signaling Technology, Danvers, MA), NG2 primary antibody (1:1,000; Millipore, Bedford, MA), and MBP primary antibody (1:500; Abcam, Cambridge, UK). Housekeeping protein, glyceraldehyde-3-phosphate dehydrogenase (1:1,000; Santa Cruz Biotechnology, Santa Cruz, CA), level was measured as a loading control, followed by secondary antibody incubation with HRP-conjugated secondary antibody (1:1,000; DAKO, Glostrup, Denmark). Detailed materials and methods for electrophoresing protein, analyzing carbonylated protein and measuring levels of probed proteins are provided in the **Supplementary Methods** online.

Superoxide Dismutase Activity

Detailed materials and methods for measuring brain SOD activity are provided in the **Supplementary Methods** online.

Functional Behavioral Tests

On the P14, negative geotaxis test (35), which assesses the innate reflex rotation to face uphill when placed head-down on an inclined wooden platform was performed. Righting reflex (42) was assessed at P11–13. Detailed materials and methods for performing these functional behavioral tests are provided in the **Supplementary Methods** online.

Brain Donor Cell Detection

Presence of intratracheally transplanted MSCs was determined by performing RT-PCR for human DNA, which was derived from transplanted human MSCs; detailed material and methods are provided in the **Supplementary Methods** online.

Statistical Analysis

Data are expressed as mean ± SEM. Given that group sizes were small, statistical differences between groups were established using the Kruskal–Wallis test, followed by Nemenyi *post hoc* analysis. Correlations between lung and brain data were analyzed using Spearman's or Pearson's correlation coefficients, as appropriate. All data were analyzed using SAS 9.4 software (SAS Institute, Cary, NC) and P values less than 0.05 were considered statistically significant.

SUPPLEMENTARY MATERIAL

Supplementary material is linked to the online version of the paper at http://www.nature.com/pr

ACKNOWLEDGMENTS

We would like to thank Hee Jin Kim, Department of Biology, Massachusetts Institute of Technology, for her assistance with animal experiments and manuscript preparation.

STATEMENT OF FINANCIAL SUPPORT

This work was supported by a Korea Research Foundation grant from the National Research Foundation of Korea (NRF) and the Ministry of Education, Science, and Technology (NRF-2014R1A1A2056427).

Disclosure: Samsung Medical Center and MEDIPOST Co., Ltd. own issued or filed patents for "Method of treating lung diseases using cells separated or proliferated from umbilical cord blood" in the names of the inventors, Y.S.C., W.S.P., and Y.S.Y.

REFERENCES

1. Ratner V, Kishkurno SV, Slinko SK, et al. The contribution of intermittent hypoxemia to late neurological handicap in mice with hyperoxia-induced lung injury. Neonatology 2007;92:50–8.
2. Anderson PJ, Doyle LW. Neurodevelopmental outcome of bronchopulmonary dysplasia. Semin Perinatol 2006;30:227–32.
3. Dammann O, Leviton A, Bartels DB, Dammann CE. Lung and brain damage in preterm newborns. Are they related? How? Why? Biol Neonate 2004;85:305–13.
4. Pham H, Vottier G, Pansiot J, et al. Inhaled NO prevents hyperoxia-induced white matter damage in neonatal rats. Exp Neurol 2014;252:114–23.
5. Chang YS, Choi SJ, Ahn SY, et al. Timing of umbilical cord blood derived mesenchymal stem cells transplantation determines therapeutic efficacy in the neonatal hyperoxic lung injury. PLoS One 2013;8:e52419.
6. Chang YS, Choi SJ, Sung DK, et al. Intratracheal transplantation of human umbilical cord blood-derived mesenchymal stem cells dose-dependently attenuates hyperoxia-induced lung injury in neonatal rats. Cell Transplant 2011;20:1843–54.
7. Chang YS, Oh W, Choi SJ, et al. Human umbilical cord blood-derived mesenchymal stem cells attenuate hyperoxia-induced lung injury in neonatal rats. Cell Transplant 2009;18:869–86.
8. Chang YS, Ahn SY, Yoo HS, et al. Mesenchymal stem cells for bronchopulmonary dysplasia: phase 1 dose-escalation clinical trial. J Pediatr 2014;164:966–972.e6.
9. Liu Y, Silverstein FS, Skoff R, Barks JD. Hypoxic-ischemic oligodendroglial injury in neonatal rat brain. Pediatr Res 2002;51:25–33.
10. Fan LW, Chen RF, Mitchell HJ, et al. alpha-Phenyl-n-tert-butyl-nitrone attenuates lipopolysaccharide-induced brain injury and improves neurological reflexes and early sensorimotor behavioral performance in juvenile rats. J Neurosci Res 2008;86:3536–47.
11. Hermans RH, Hunter DE, McGivern RF, Cain CD, Longo LD. Behavioral sequelae in young rats of acute intermittent antenatal hypoxia. Neurotoxicol Teratol 1992;14:119–29.
12. Trittmann JK, Nelin LD, Klebanoff MA. Bronchopulmonary dysplasia and neurodevelopmental outcome in extremely preterm neonates. Eur J Pediatr 2013;172:1173–80.
13. Sirinyan M, Sennlaub F, Dorfman A, et al. Hyperoxic exposure leads to nitrative stress and ensuing microvascular degeneration and diminished brain mass and function in the immature subject. Stroke 2006;37:2807–15.
14. Felderhoff-Mueser U, Bittigau P, Sifringer M, et al. Oxygen causes cell death in the developing brain. Neurobiol Dis 2004;17:273–82.
15. Gerstner B, DeSilva TM, Genz K, et al. Hyperoxia causes maturation-dependent cell death in the developing white matter. J Neurosci 2008;28:1236–45.
16. Anjari M, Counsell SJ, Srinivasan L, et al. The association of lung disease with cerebral white matter abnormalities in preterm infants. Pediatrics 2009;124:268–76.
17. Zaghloul N, Nasim M, Patel H, et al. Overexpression of extracellular superoxide dismutase has a protective role against hyperoxia-induced brain injury in neonatal mice. FEBS J 2012;279:871–81.
18. Brehmer F, Bendix I, Prager S, et al. Interaction of inflammation and hyperoxia in a rat model of neonatal white matter damage. PLoS One 2012;7:e49023.
19. Gray PH, O'Callaghan MJ, Rogers YM. Psychoeducational outcome at school age of preterm infants with bronchopulmonary dysplasia. J Paediatr Child Health 2004;40:114–20.
20. Chang YS, Ahn SY, Jeon HB, et al. Critical role of vascular endothelial growth factor secreted by mesenchymal stem cells in hyperoxic lung injury. Am J Respir Cell Mol Biol 2014;51:391–9.
21. Gerstner B, Bührer C, Rheinländer C, et al. Maturation-dependent oligodendrocyte apoptosis caused by hyperoxia. J Neurosci Res 2006;84:306–15.
22. Vottier G, Pham H, Pansiot J, et al. Deleterious effect of hyperoxia at birth on white matter damage in the newborn rat. Dev Neurosci 2011;33:261–9.
23. Back SA. Perinatal white matter injury: the changing spectrum of pathology and emerging insights into pathogenetic mechanisms. Ment Retard Dev Disabil Res Rev 2006;12:129–40.
24. Khan JY, Black SM. Developmental changes in murine brain antioxidant enzymes. Pediatr Res 2003;54:77–82.
25. Blomgren K, Hagberg H. Free radicals, mitochondria, and hypoxia-ischemia in the developing brain. Free Radic Biol Med 2006;40:388–97.
26. D'Amelio M, Cavallucci V, Cecconi F. Neuronal caspase-3 signaling: not only cell death. Cell Death Differ 2010;17:1104–14.
27. Watson RE, Desesso JM, Hurtt ME, Cappon GD. Postnatal growth and morphological development of the brain: a species comparison. Birth Defects Res B Dev Reprod Toxicol 2006;77:471–84.
28. Haorah J, Knipe B, Leibhart J, Ghorpade A, Persidsky Y. Alcohol-induced oxidative stress in brain endothelial cells causes blood-brain barrier dysfunction. J Leukoc Biol 2005;78:1223–32.
29. Stolp HB, Dziegielewska KM, Ek CJ, et al. Breakdown of the blood-brain barrier to proteins in white matter of the developing brain following systemic inflammation. Cell Tissue Res 2005;320:369–78.
30. Wei X, Du Z, Zhao L, et al. IFATS collection: The conditioned media of adipose stromal cells protect against hypoxia-ischemia-induced brain damage in neonatal rats. Stem Cells 2009;27:478–88.
31. Porzionato A, Macchi V, Zaramella P, et al. Effects of postnatal hyperoxia exposure on the rat dentate gyrus and subventricular zone. Brain Struct Funct 2015;220:229–47.
32. Wise SP, Boussaoud D, Johnson PB, Caminiti R. Premotor and parietal cortex: corticocortical connectivity and combinatorial computations. Annu Rev Neurosci 1997;20:25–42.
33. Felderhoff-Mueser U, Sifringer M, Polley O, et al. Caspase-1-processed interleukins in hyperoxia-induced cell death in the developing brain. Ann Neurol 2005;57:50–9.

34. Ramani M, van Groen T, Kadish I, Bulger A, Ambalavanan N. Neurodevelopmental impairment following neonatal hyperoxia in the mouse. Neurobiol Dis 2013;50:69–75.
35. Ahn SY, Chang YS, Sung DK, et al. Mesenchymal stem cells prevent hydrocephalus after severe intraventricular hemorrhage. Stroke 2013;44:497–504.
36. Ahn SY, Chang YS, Sung DK, et al. Optimal route for mesenchymal stem cells transplantation after severe intraventricular hemorrhage in newborn rats. PLoS One 2015;10:e0132919.
37. Sung DK, Chang YS, Ahn SY, et al. Optimal route for human umbilical cord blood-derived mesenchymal stem cell transplantation to protect against neonatal hyperoxic lung injury: gene expression profiles and histopathology. PLoS One 2015;10:e0135574.
38. Mahmood A, Lu D, Wang L, Li Y, Lu M, Chopp M. Treatment of traumatic brain injury in female rats with intravenous administration of bone marrow stromal cells. Neurosurgery 2001;49:1196–203; discussion 1203–4.
39. Dalous J, Pansiot J, Pham H, et al. Use of human umbilical cord blood mononuclear cells to prevent perinatal brain injury: a preclinical study. Stem Cells Dev 2013;22:169–79.
40. Kitamura M, Itoh K, Matsumoto A, et al. Prenatal ionizing radiation-induced apoptosis of the developing murine brain with special references to the expression of some proteins. Kobe J Med Sci 2001;47:59–76.
41. Cooney TP, Thurlbeck WM. The radial alveolar count method of Emery and Mithal: a reappraisal 2–intrauterine and early postnatal lung growth. Thorax 1982;37:580–3.
42. Bassan H, Bassan M, Pinhasov A, et al. The pregnant spontaneously hypertensive rat as a model of asymmetric intrauterine growth retardation and neurodevelopmental delay. Hypertens Pregnancy 2005;24:201–11.